Transonic Aeroelasticity Analysis Using State-Space Unsteady Aerodynamic Modeling

G. L. Crouse Jr.* and J. G. Leishman†
University of Maryland, College Park, Maryland 20742

An aeroelastic analysis is conducted on a two-degree-of-freedom airfoil in transonic flow using a generalized state-space approximation for the unsteady aerodynamics. The aerodynamic representation is validated against computational fluid dynamic solutions for angle of attack oscillations up to Mach numbers of 0.875 and at reduced frequencies up to 1.0. Despite the inherent nonlinear nature of transonic flow, it is shown that a linear finite-state model with as few as eight states can provide a good approximation to the unsteady lift and moment behavior if appropriate allowance is made for Mach number effects on the airfoil's static lift curve slope and mean aerodynamic center. It is shown how the aerodynamic representation can be coupled to the structural equations of a typical airfoil section with bending and torsional degrees of freedom. The stability of the resulting aeroelastic system is determined by eigenanalysis. This aeroelastic analysis is shown to be in excellent agreement with calculations performed using more sophisticated unsteady aerodynamic theories.

Nomenclature

A_n = coefficients of indicial functions
a = sonic velocity
b = semichord, $c/2$
b_n = exponents of indicial functions
C_M = pitching moment about the ¼-chord
C_N = normal force coefficient
$C_{N\alpha}$ = normal force curve slope
c = airfoil chord
g_h, g_θ = structural damping in plunging and pitching, respectively
h = plunge (bending) displacement, positive downward
I_θ = polar moment of inertia about ¼-chord per unit length
K_h, K_θ = spring stiffness in bending and torsion, respectively
k = reduced frequency, $\omega c/2V$
M = Mach number
m = mass per unit length
Q_h, Q_θ = generalized aerodynamic forces in plunging and pitching, respectively
q = nondimensional pitch rate, $\dot{\alpha}c/V$
r_θ = radius of gyration about elastic axis, $\sqrt{I_\theta/mb^2}$
S = distance traveled in semichords, $2Vt/c$
S_θ = static mass moment, mbx_θ
T_I = basic noncirculatory time constant, c/a
t = time
V = freestream velocity
x_{ac} = nondimensional position of the aerodynamic center measured from the leading edge
x_i = state variable
x_θ = nondimensional distance in semichords from elastic axis to center of mass
α = angle of attack
β = compressibility factor, $\sqrt{1-M^2}$
θ = pitch angle
λ = eigenvalue
μ = airfoil mass ratio, $m/\rho\pi b^2$
ρ = air density
ϕ = indicial response function
ω_h = uncoupled bending frequency, $\sqrt{K_h/m}$
ω_θ = uncoupled torsion frequency, $\sqrt{K_\theta/I_\theta}$

Subscripts
M = pitching moment about the ¼ chord
q = pitch rate
α = angle of attack

Superscripts
C = circulatory component
I = noncirculatory (impulsive) component

I. Introduction

THE calculation of the aeroelastic response of lifting surfaces operating in the transonic flow range is of considerable importance in aircraft design. Many aircraft operate in transonic flow during at least part of their flight envelope, and the avoidance of transonic flutter is an important consideration. The main problem is that under transonic flow conditions, small displacements of the airfoil section will produce large changes in the aerodynamic forces and pitching moments about the elastic axis. Furthermore, under time-dependent conditions, considerable phase differences can exist between the airfoil motion and the resultant airloads. These unsteady aerodynamic characteristics often make aeroelastic instabilities and flutter more likely to occur on lifting surfaces when transonic flow conditions exist. Unsteady transonic aerodynamics is also of great concern in helicopters, since in forward flight the advancing blade tip may penetrate well into the transonic region.

Aeroelastic analyses are typically concerned with finding all the likely instabilities of a given configuration, or finding the variation of flutter speed with certain key structural parameters. These analyses are usually performed repeatedly to optimize the final design. As a result, there is considerable motivation to be able to perform aeroelastic calculations quickly and inexpensively. For rotorcraft analyses, the incentive is even greater because the complex nature of both the flowfield and the blade dynamics makes the aeroelastic analysis considerably more time consuming than for fixed wing aircraft.

Presented in part as Paper 89-0022 at the AIAA 27th Aerospace Sciences Meeting, Reno, NV, Jan. 9–12, 1989; received May 16, 1989; revision received Nov. 28, 1990; accepted for publication Jan. 3, 1991. Copyright © 1991 by the American Institute of Aeronautics and Astronautics, Inc. All rights reserved.

*Rotorcraft Fellow, Department of Aerospace Engineering. Student Member AIAA.

†Assistant Professor, Department of Aerospace Engineering. Member AIAA.

All aeroelastic analyses are greatly simplified when the governing aerodynamic equations can be linearized. If the aerodynamics can be treated in a linear manner then classical theory is readily available for the aeroelastician's use, see, for example, Refs. 1 and 2. Under purely subsonic or supersonic flow conditions, the governing flow equations are linear and the aerodynamic forces and moments depend on the airfoil motion in a linear manner. However, under transonic flow conditions, the governing aerodynamic equations become inherently nonlinear. The nonlinearities manifest themselves through changes in the airfoil pressure distribution via the shock wave strength and position and, consequently, on the resultant forces and moments. These effects can be represented completely only by a method that can solve the governing nonlinear flow equations. As a result, the representation of the unsteady aerodynamic effects in a form suitable for routine transonic aeroelasticity calculations generally proves difficult.

Currently, the most accurate aerodynamic models for transonic flow are computational fluid dynamic (CFD) solutions to the governing equations. A state-of-the-art review of CFD methods for determining the transonic flowfield around two-dimensional airfoils is given by Ballhaus and Bridgeman.[3] The first use of a CFD method (LTRAN2) in a time-marching transonic flutter prediction was performed by Ballhaus and Goorjian,[4] and recent transonic aeroelasticity studies have essentially continued along these lines.[4–7] These CFD-based approaches are often considered to be the salvation of the aeroelastician; however, in many situations, a time-marching aeroelastic analysis using a CFD method is very computationally expensive for routine design purposes or parametric studies, particularly so in the case of rotors.

The limitations of a time-marching aeroelastic analysis are compounded by the fact that little direct information is obtained on the damping of the aeroelastic system. Usually, an analysis must be performed on the time history of the response to obtain the natural frequencies and mode shapes. The determinations of the aeroelastic stability boundaries can thus require extensive amounts of computer resources. Hence, for many practical studies of aeroelasticity involving transonic flow, an alternative and much simplified representation of the unsteady aerodynamic behavior of the airfoil sections is extremely useful if it can be properly justified.

Many transonic aeroelasticity analyses have assumed linearity for the airloads so that traditional linear flutter methods can be used, for example, Refs. 4, 6, 8, and 9. A lucid discussion of when the aerodynamic forces may be linearized in transonic flow is given by Dowell et al.[10] Generally, in transonic flow, linearity can be assumed readily if the angle-of-attack displacements are moderately small or if the reduced frequency is either very low or relatively high. Current linearized methods generally utilize oscillatory unsteady aerodynamic coefficients obtained from panel methods or CFD solutions to construct approximate solutions for the generalized airloads. For example, Refs. 9 and 11 are typical in which Padé interpolating functions are used. The addition of the resulting expressions for the airloads to the structural equations of motion then produces a matrix of equations in state-space form, which can then be directly used for stability analyses of the wing. However, identification of the aerodynamic states in this manner for rotor aeroelasticity is difficult or impossible because of the varying Mach number with both blade station and azimuth angle, coupled with the more complex wake structure. Thus, the aerodynamic states for use in rotor aeroelasticity must be obtained from two-dimensional aerodynamic theories, and the unsteady aerodynamic approximation generalized wherever possible in terms of section Mach number.

It is the objective of this work to describe an approximate, but fairly general and efficient time-domain method for performing aeroelasticity analysis in both subsonic and transonic Mach number ranges. The model starts with generalized approximate forms of the indicial lift and pitching moment functions for a typical section in compressible flow.[14] From these, a set of first-order ordinary differential equations (ODEs) are derived, which relate the airfoil motion to the airloads. The resulting first-order ODEs describing the unsteady aerodynamics can then be appended readily to the structural response equations governing the airfoil dynamics.

To support the development of the method, illustrative examples are presented for the unsteady lift and pitching moment on a two-dimensional airfoil undergoing oscillatory forcing in transonic flow and are compared with results computed by CFD codes. The aerodynamic theory is also combined with the structural equations of motion of an airfoil section with pitch and plunge degrees of freedom. The ability to efficiently and accurately compute the flutter speed of the airfoil is demonstrated using direct eigenanalysis of the state equations.

II. Methodology

A. Aerodynamic Approximation

The unsteady aerodynamic behavior of a two-dimensional airfoil can be approximately described using a finite set of n first-order ODEs of the form

$$\dot{x} = Ax + Bu \tag{1}$$

with p output equations

$$y = Cx + Du \tag{2}$$

where $\dot{x} = dx/dt$; $u = u_i$, $i = 1,2, \ldots, m$ are the system inputs (i.e., angle of attack and pitch rate), and the $y = y_i$, $i = 1,2, \ldots, p$ are the system outputs (i.e., the forces and moments). $x = x_i$, $i = 1,2, \ldots, n$ are the aerodynamic state variables. The aerodynamic states provide the information required at a given instant in time to allow the determination of the future airloads given future inputs in airfoil motion. In general, a minimum number of states must be used to economize on computational resources.

To obtain a finite number of aerodynamic state equations, one can work with suitable representations of the indicial response functions in a convenient approximate form. Wagner[15] has obtained the indicial lift response of an airfoil operating in incompressible flow, the result of which is expressed in terms of Bessel functions. Since this is not particularly convenient, Jones' exponential approximation[16] to the Wagner function is typically used in the analysis of both fixed wing and rotary wing aeroelasticity problems. For example, Edwards et al.[17] show how a state-space representation for the incompressible flow regime can be derived from Jones' approximation to the Wagner function. The use of an incompressible aerodynamic theory is, however, of limited practical utility in the aeroelastic analysis of wing systems at higher Mach numbers where significant compressibility effects become increasingly important.

Although there is no exact equivalent to the Wagner function for compressible flow, an approximation can be derived by using certain generalizations to include the effects of compressibility. Beddoes[18] recently derived a generalized exponential series approximation for subsonic indicial response functions, and this work has been extended and validated by Leishman[14] using a variety of experimental and theoretical results. The state equations describing the unsteady aerodynamic response can be obtained by direct application of Laplace transforms to these indicial response functions.[12,13]

The indicial response functions can be represented adequately by exponential approximations with up to three terms. Experience has shown that this level of approximation is adequate if care is taken when selecting the values of the exponential coefficients. To place a physical significance on the phenomena occurring during the indicial response, the approximating functions are idealized into two parts. The first

part of the response is for the noncirculatory loading, which represents the time-dependent airloads due to acoustic wave propagation. The noncirculatory part was first extracted by Mazelsky[19] and later approximated by Beddoes.[18] The initial value of this loading is derived from piston theory[2] and is valid for any Mach number. For subsequent time, these initial pressure waves propagate at the local speed of sound and the loading quickly decays from its initial value. The second part of the indicial response is due to the circulatory loading that builds up asymptotically to the steady-state value as the shed wake is convected downstream from the airfoil.

In general, the indicial normal force response to a step change in angle of attack α can be written as

$$\frac{C_N(S)}{\alpha} = \frac{4}{M}\phi_\alpha^I(S, M) + C_{N_\alpha}(M)\phi_\alpha^C(S, M) \tag{3}$$

where the indicial responses ϕ_α^C, ϕ_α^I are exponential functions that are expressed in terms of both aerodynamic time S and the Mach number M.

The indicial functions ϕ_α^C and ϕ_α^I due to angle of attack α can be written

$$\phi_\alpha^C(S, M) = 1 - A_1 \exp(-b_1\beta^2 S) - A_2 \exp(-b_2\beta^2 S) \tag{4}$$

and

$$\phi_\alpha^I(S, M) = \exp\left(\frac{-S}{T_\alpha}\right) \tag{5a}$$

or

$$\phi_\alpha^I(t, M) = \exp\left(\frac{-t}{K_\alpha T_I}\right) \tag{5b}$$

The form of ϕ_α^C is very similar to Jones' approximation to the Wagner function, however, the empirically derived constants used here have the values $A_1 = 0.3$, $A_2 = 0.7$, $b_1 = 0.14$, $b_2 = 0.53$ and the exponents are scaled with β^2, as given in Ref. 18. K_α is an analytical function of Mach number and the coefficients A_1, A_2, b_1, and b_2 are as derived in Ref. 14, with $T_I = c/a$. Furthermore, the circulatory loads are dependent on the lift curve slope C_{N_α}, which is a function of Mach number and can be obtained from experimental measurements or, more approximately, by using a simple Prandtl-Glauert type compressibility correction to the low Mach number results.

The typical behavior of the indicial lift response for a step change in angle of attack is shown in Fig. 1 for a Mach number of 0.8 in comparison with results published by Magnus[20] for the indicial response in transonic flow using an Euler code.

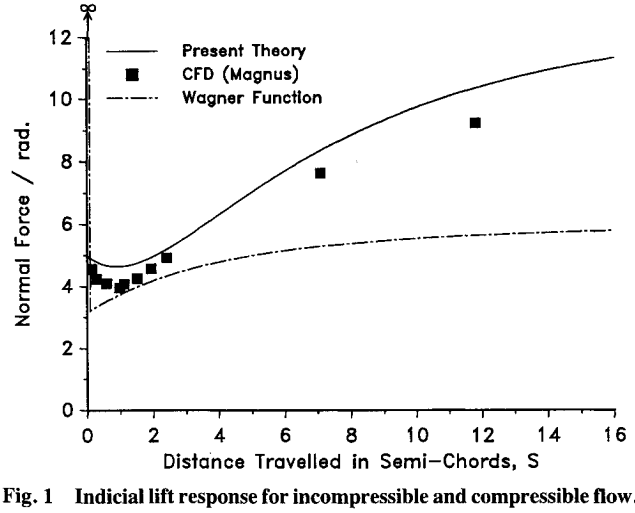

Fig. 1 Indicial lift response for incompressible and compressible flow.

Also shown in Fig. 1 for reference is the classical Wagner function, which, in contrast to the compressible functions, has an infinite value at $S = 0$. The lift curve slope used in the present approximation to the compressible indicial response was derived from Magnus' asymptotic value to allow a direct comparison. The comparison is quite good and gives considerable confidence in the approximating functions used here for the indicial response at transonic Mach numbers.

Starting from these approximations to the indicial functions, the normal force response to changes in the angle of attack can be derived in the state-space form. The first two states (associated with the lags b_1 and b_2) represent, in aggregate, how the shed wake affects the circulatory component of the normal force. This part can be written as

$$\begin{bmatrix}\dot{x}_1\\ \dot{x}_2\end{bmatrix} = \left(\frac{2V}{c}\right)\beta^2\begin{bmatrix}-b_1 & 0\\ 0 & -b_2\end{bmatrix}\begin{bmatrix}x_1\\ x_2\end{bmatrix} + \begin{bmatrix}1\\ 1\end{bmatrix}\alpha_{3/4}(t) \tag{6}$$

with the output equation for the normal force coefficient given by

$$C_N^C(t) = C_{N_\alpha}(M)\left(\frac{2V}{c}\right)\beta^2\begin{bmatrix}A_1b_1 & A_2b_2\end{bmatrix}\begin{bmatrix}x_1\\ x_2\end{bmatrix} \tag{7}$$

where, in accordance with the thin airfoil approximation, $\alpha_{3/4}$ is the quasisteady angle of attack at the $\frac{3}{4}$-chord, i.e.,

$$\alpha_{3/4}(t) = \alpha(t) + \frac{q(t)}{2} \tag{8}$$

The third state is a result of the time-dependent noncirculatory loads, and this contribution can be written in the state-space form as

$$\dot{x}_3 = -\frac{1}{K_\alpha T_I}x_3 + \alpha(t) \tag{9}$$

$$C_N^I(t) = \frac{4}{M}\left[-\frac{1}{K_\alpha T_I}x_3 + \alpha(t)\right] \tag{10}$$

where $K_\alpha T_I$ is the time constant associated with the loss of lift due to acoustic wave propagation.

In a similar manner, the $\frac{1}{4}$-chord pitching moment response to a step change in angle of attack α can be written as

$$\frac{C_M(S)}{\alpha} = -\frac{1}{M}\phi_{\alpha M}^I(S, M) + C_{N_\alpha}(M)\phi_\alpha^C(S, M)[0.25 - x_{ac}(M)] \tag{11}$$

The indicial response $\phi_{\alpha M}^I$ is written in a manner analogous to ϕ_α^I, but represents the noncirculatory contribution to the pitching moment. The second term in Eq. (11) represents the circulatory contribution to the pitching moment due to a Mach number dependent offset of the aerodynamic center x_{ac} from the airfoil $\frac{1}{4}$-chord axis. The value of x_{ac} is dependent on airfoil section and Mach number. Normally, this could be obtained either from experimental airfoil data or from CFD analysis under stated conditions. At low subsonic speeds, the aerodynamic center lies close to the $\frac{1}{4}$-chord, although, for transonic speeds, the effective aerodynamic center moves quickly to the vicinity of the $\frac{1}{2}$-chord as the freestream Mach number increases, a result not predicted by linearized theory.

The complete equations for the normal force and pitching moment due to changes in angle of attack α and pitch rate q are derived in Refs. 12 and 13. This produces an eight-state model for the circulatory and noncirculatory components of the unsteady lift and pitching moment. The individual components of aerodynamic loading are then summed in a linear manner to obtain the net aerodynamic response. Thus, the

aerodynamic model can be expressed in terms of a two-input, two-output system where the inputs are the angle of attack and pitch rate (α, q) and the outputs are the unsteady normal force (lift) and pitching moment coefficients (C_N, C_M). The complete set of eight-state equations representing the aerodynamics are

$$\dot{x} = Ax + B\begin{Bmatrix}\alpha\\ q\end{Bmatrix} \tag{12a}$$

$$\begin{Bmatrix}C_N\\ C_M\end{Bmatrix} = Cx + D\begin{Bmatrix}\alpha\\ q\end{Bmatrix} \tag{12b}$$

These matrices are fully defined in Ref. 13. Note that the only free parameters in this representation are the static lift curve slope and the aerodynamic center offset from the ¼-chord.

B. State-Space Aeroelastic Model

With these generalized unsteady aerodynamic equations written in a first-order state-space form, they can be coupled into the equations of motion of an airfoil section with bending and torsion degrees of freedom. The parameters and sign conventions for a typical airfoil section are shown in Fig. 2. The equations of motion can be written in terms of the inertia forces, elastic forces, and aerodynamic forces as

$$m\ddot{h} + S_\theta\ddot{\theta} + g_h\dot{h} + m\omega_h^2 h = Q_h \tag{13a}$$

$$S_\theta\ddot{h} + I_\theta\ddot{\theta} + g_\theta\dot{\theta} + I_\theta\omega_\theta^2\theta = Q_\theta \tag{13b}$$

Written in matrix form, these equations become

$$m\ddot{u} + g\dot{u} + ku = Q \tag{14}$$

where

$$m = \begin{bmatrix}m & S_\theta\\ S_\theta & I_\theta\end{bmatrix} \qquad g = \begin{bmatrix}g_h & 0\\ 0 & g_\theta\end{bmatrix}$$

$$k = \begin{bmatrix}m\omega_h^2 & 0\\ 0 & I_\theta\omega_\theta^2\end{bmatrix} \qquad u = \begin{Bmatrix}h\\ \theta\end{Bmatrix}$$

$$Q = \begin{Bmatrix}-L\\ M\end{Bmatrix} = \frac{1}{2}\rho V^2\begin{bmatrix}-c & 0\\ 0 & c^2\end{bmatrix}\begin{Bmatrix}C_N\\ C_M\end{Bmatrix}$$

This set of second-order differential equations can be converted to first-order form by defining the states

$$z_1 = h, \qquad z_2 = \theta, \qquad z_3 = \dot{h}, \qquad z_4 = \dot{\theta} \tag{15}$$

The structural dynamic equations then become

$$\begin{bmatrix}\mathrm{I} & 0\\ 0 & m\end{bmatrix}\dot{z} = \begin{bmatrix}0 & I\\ -k & -g\end{bmatrix}z + \begin{Bmatrix}0\\ Q\end{Bmatrix} \tag{16}$$

It should be noted that the main differences between the various methods that exist for aeroelasticity analysis lie within the prediction of the aerodynamic loads Q. For a quasisteady aerodynamic representation, Q can be expressed in terms of the instantaneous displacements z alone. In practice, however, both the circulatory and noncirculatory airloads depend on the *time histories* of the pitch angle displacement θ and the derivatives $\dot{\theta}$ and $\dot{h}$.

In order to couple the structural and aerodynamic equations, the unsteady aerodynamic equations given previously can be expressed in terms of the z states as

$$\dot{x} = Ax + B'z \tag{17}$$

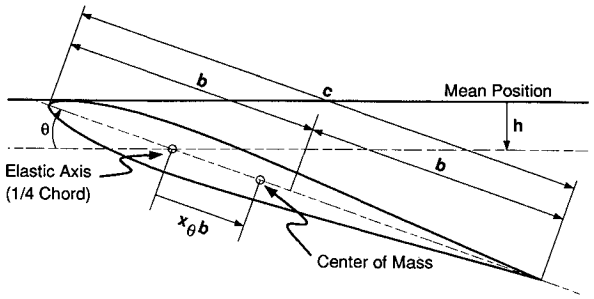

Fig. 2 Definition of parameters for a two-degree-of-freedom airfoil section.

where B' is an 8 × 4 matrix and

$$Q = \frac{1}{2}\rho V^2\begin{bmatrix}-c & 0\\ 0 & c^2\end{bmatrix}\begin{Bmatrix}C_N\\ C_M\end{Bmatrix} = C'x + [D_1'D_2']z \tag{18}$$

The matrices B', C', D_1', D_2' correspond to the matrices B, C, and D, that were introduced in Eq. (12), however, the prime indicates that those matrices have been multiplied by a constant. In addition, the D matrix has been separated into two matrices, D_1' and D_2'.

These equations for the unsteady airloads can be coupled into the structural equations to give the final equations of the aeroelastic system

$$\begin{bmatrix}I & 0 & 0\\ 0 & M & 0\\ 0 & 0 & I\end{bmatrix}\begin{Bmatrix}\dot{z}\\ \dot{x}\end{Bmatrix} = \begin{bmatrix}0 & I & 0\\ D_1' - k & D_2' - g & C'\\ B' & & A\end{bmatrix}\begin{Bmatrix}z\\ x\end{Bmatrix} \tag{19}$$

which is a 12 × 12 system of linear equations. The 2 × 2 aerodynamic matrices D_1' and D_2' contain the initial values of the indicial response functions (the piston theory terms), and it can be shown that these terms are in fact associated with both the stiffness and damping terms in the aeroelastic system. The matrix A is the 8 × 8 aerodynamic state matrix given in Eq. (12). This is the aerodynamic feedback matrix for the system that is responsible for the time history effects (both circulatory and noncirculatory) on the aerodynamic loading. When using incompressible theory (Jones' approximation to the Wagner function), a similar system of equations is produced, but only six linear equations are required.

The aeroelastic stability of the system is determined by a 12 × 12 eigenvalue problem, which yields the eigenvalues $\lambda_k = \sigma_k + i\omega_k$. For any $\sigma_k > 0$, the system is unstable. Alternatively, Eq. (19) may be directly integrated with respect to time using a standard ODE solver and the response simply monitored for converging or diverging behavior.

III. Results and Discussion

The aerodynamic method presented here requires as input the static lift curve slope and the aerodynamic center offset from the ¼-chord for each airfoil under consideration. These data are readily available for most airfoils in the subsonic and transonic region. In this paper, we confine our attention to the well-used NACA 64A006 airfoil for which experimental data are available in Ref. 21. In addition, Yang et al.[22] present data for static conditions as obtained from two transonic small disturbance (TSD) codes, namely, LTRAN2-NLR and STRANS2/UTRANS2. Figure 3 presents the results of these two codes, the experimental measurements, and also the lift curve slope using the Prandtl-Glauert correction. The variations shown in Fig. 3 clearly indicate the well-known rapid increase in the lift curve slope and the corresponding aft movement of x_{ac} with increasing subsonic Mach number.

The validity of the present unsteady aerodynamic approximations under transonic flow conditions has been investigated by comparing with various CFD solutions for the in-

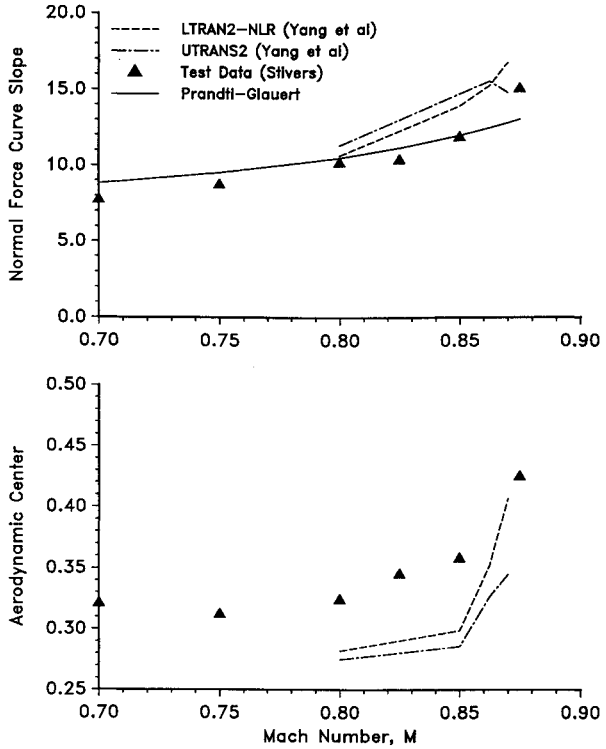

Fig. 3 Variation of lift curve slope and aerodynamic center with Mach number for the NACA 64A006 airfoil.

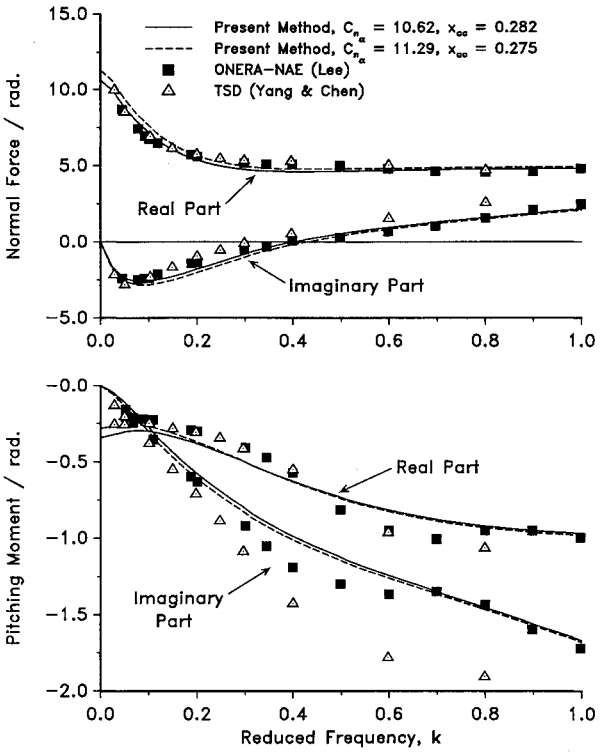

Fig. 4 Variation of lift and pitching moment for extended reduced-frequency range at $M = 0.8$.

viscid transonic flow about unsteady airfoils. One such comparison is shown in Fig. 4 for the unsteady lift and pitching moment on a NACA 64A006 airfoil during a harmonic pitch oscillation at $M = 0.8$. The CFD data were computed by Lee[23] using a modified ONERA TSD code in which high-frequency terms (the second time derivative) have been retained in the governing equations. For convenience, this code is referred to as the ONERA-NAE code. The particular data computed by Lee[23] are quite unique since the unsteady aerodynamic loads at reduced frequencies ($k = \omega c/2V$) up to 1.0 were obtained. This is significantly higher than can be obtained experimentally. Also shown in Fig. 4 are TSD results computed by Yang and Chen[24]; however, because these results were not computed with the second time derivative, they probably cannot be considered as accurate as those computed by Lee.

As demonstrated in Fig. 4, the accuracy of the present unsteady aerodynamic approximations in predicting both the normal force (lift) and pitching moment over the full reduced-frequency range is highly encouraging. It should be noted that both angle of attack and pitch rate terms are included. The asymptotic behavior of the lift and moment at high reduced frequencies is dominated by the noncirculatory aerodynamic loading and is consistent with the values predicted using piston theory. Further results (not shown) for the lift response for both pitch and plunge oscillations were found to be in good agreement with the ONERA-NAE data over a range of Mach numbers from 0.8 up to 0.875.

The behavior of the unsteady pitching moment is often more critical to flutter and is quite difficult to predict accurately in transonic flow. The unsteady pitching moment is shown in Fig. 5 vs reduced frequency for Mach numbers of 0.85 and 0.875. At $M = 0.8$, the flow about the NACA 64A006 airfoil is essentially shockless, although at $M = 0.85$, a shock wave forms intermittently on the airfoil (Tijdeman B-type shock development[25]). It is noteworthy that the shock displacement (and the associated pressure changes) significantly lag the airfoil motion and result in large excursions in pitching moment at values of k around 0.35. Even so, this nonlinear behavior is confined to a narrow frequency range and disappears as the reduced frequency increases further and the shock wave position stabilizes. At a Mach number of 0.875, a shock wave is fully developed on the airfoil and the x_{ac} moves significantly aft of the $\frac{1}{4}$-chord. It should be noted that the shock wave displacement is actually quite large for low-frequency oscillations; nevertheless, the present method does fairly well in predicting both the real and the imaginary components of the resulting pitching moment response.

The correlations obtained in Figs. 4 and 5 lend considerable confidence to the ability of the present method to accurately

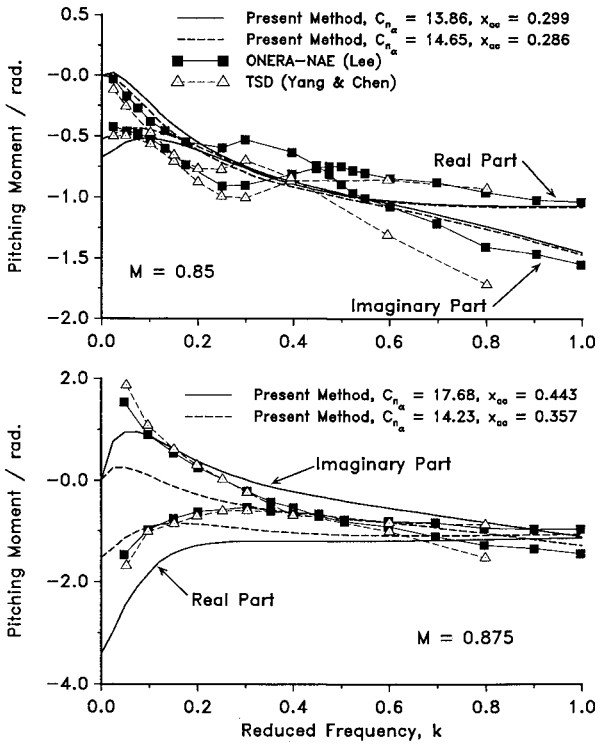

Fig. 5 Variation of aerodynamic pitching moment for extended reduced-frequency range at $M = 0.85$ and 0.875.

predict both the amplitude and phasing of the unsteady aerodynamic behavior in transonic flow. The results also essentially substantiate aerodynamic linearity for transonic flow so long as the flow remains attached to the airfoil, i.e., at low angles of attack. This has been confirmed experimentally by Davis and Malcolm[26] from wind-tunnel tests on oscillating NACA 64A006 and 64A010 airfoils.

The second part of this discussion concerns the application of the aerodynamic model to the prediction of the aeroelastic stability of a two-degree-of-freedom airfoil. This aeroelastic analysis was performed using eigenanalysis of the state equations. Many aeroelastic analyses, particularly those used in the rotorcraft industry, still use incompressible unsteady aerodynamics for its simplicity, despite the limitations when applied to higher Mach number flows. Thus, to provide a reference, a comparison was undertaken to explore the limits of classical incompressible theory. For this, Jones' approximation to the Wagner function[16] was used for the circulatory lift. The apparent mass terms[2] were also added.

Jones' approximation to the indicial lift response is given by

$$\phi(S) = 1 - 0.165 \exp(-0.0455S) - 0.335 \exp(-0.3S) \tag{20}$$

from which a state-space equation for the lift response to an arbitrary forcing can be readily written in the same manner as the compressible indicial response functions described previously in Eq. (20). The additional apparent mass forces are

$$L = \pi\rho b^2 \left[\ddot{h} + V\dot{\theta} + \frac{b}{2}\ddot{\theta} \right] \tag{21}$$

$$M = \pi\rho b^2 \left[-\frac{1}{2}\ddot{h} - V\dot{\theta} - \frac{3}{8}b\ddot{\theta} \right] \tag{22}$$

From these relations, the noncirculatory lift and pitching moment can be written as functions of the structural states only. No additional states are required to model these noncirculatory loads since they do not depend on the time history of the airfoil, as they do for compressible flow conditions. Thus, for incompressible unsteady flow, the time-varying airloads can be written as a six-state system with two inputs (α, q) and two outputs (C_N, C_M).

In order to obtain results consistent with those obtained with the compressible unsteady aerodynamics model, a Mach number dependent normal force curve slope was used, along with the corresponding aerodynamic center offset from the ¼-chord. The first results presented are at a Mach number of 0.85. From Fig. 5, it can be seen that this Mach number is typically where the largest deviations from aerodynamic linearity occur, therefore, the flutter predictions should be the most optimistic. The following mass and stiffness parameters were used: $x_\theta = 0.25$, $r_\theta = 0.5$, $\omega_h/\omega_\theta = 0.2$, pitch axis = 0.25 chord ($a_h = -0.5$), which are consistent with those used by Lee[23] and Yang et al.[22] A mass ratio of $\mu = 100$ was used, and no structural damping was included, i.e., $g_h = g_\theta = 0$.

The solution of this 12 × 12 eigenvalue problem yields the aeroelastic modes and the eigenvalues $\lambda_k = \sigma_k + i\omega_k$. For any $\sigma_k > 0$, the aeroelastic system is unstable. The corresponding damping ratio associated with each aeroelastic mode is given by

$$\zeta_k = -\sigma_k/\sqrt{\sigma_k^2 + \omega_k^2} \tag{23}$$

If any of the eigenvalues exhibit a negative damping ratio, the system is unstable.

From such an eigenanalysis, it is found that, for the conditions considered here, there are generally six highly damped aeroelastic modes and two pairs of complex conjugate eigenvalues that are associated with the structural modes. An additional complex conjugate pair appears that has a low frequency and is highly damped. This is a torsional mode that is coupled with the unsteady aerodynamics. For the particular example considered here, a root locus plot is shown in Fig. 6. With increasing velocity, the torsion branch moves directly into the stable left plane and the bending branch becomes the flutter mode.

A corresponding plot of the damping ratio vs nondimensional velocity for the bending mode is shown in Figs. 7. Results from Lee[23] are also presented along with results from classical unsteady incompressible flow theory. The present method predicts that bending flutter will occur at a nondimensional speed of $V/b\omega_\theta = 4.4$. This compares well with Lee's prediction of $V/b\omega_\theta = 4.3$. Note that unsteady incompressible flow theory gives a significantly higher flutter speed.

In Fig. 8, the flutter speed at $M = 0.85$ is computed for a range of mass ratios μ and is compared with the results of both Lee,[23] and Guruswamy and Yang.[5] The agreement is extremely good and gives considerable confidence in the utility of the present method for quantitative flutter predictions at transonic Mach numbers.

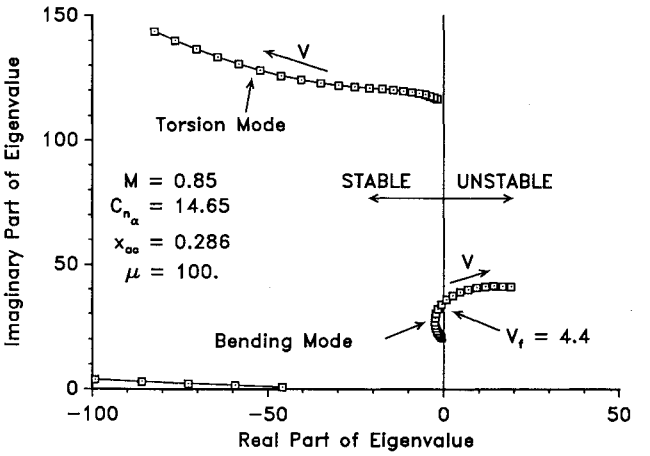

Fig. 6 Root locus plot for aeroelastic system at $M = 0.85$.

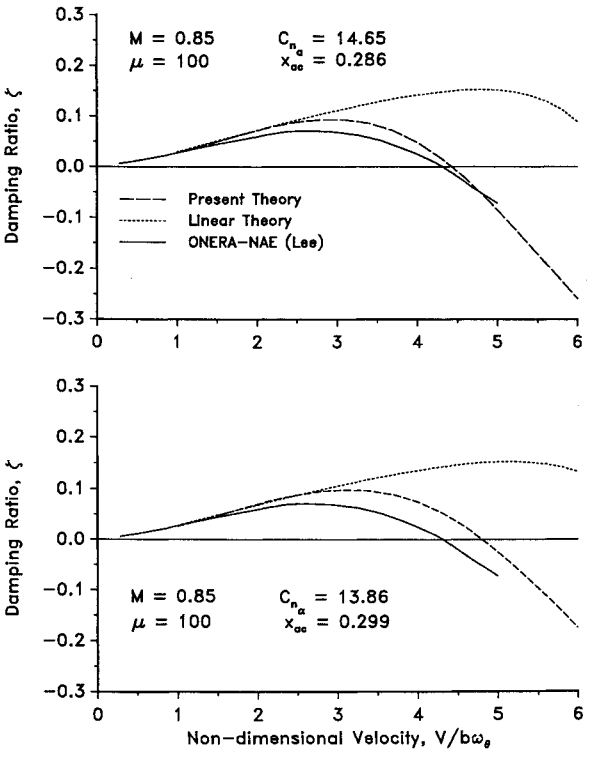

Fig. 7 Damping ratio for bending mode at $M = 0.85$.

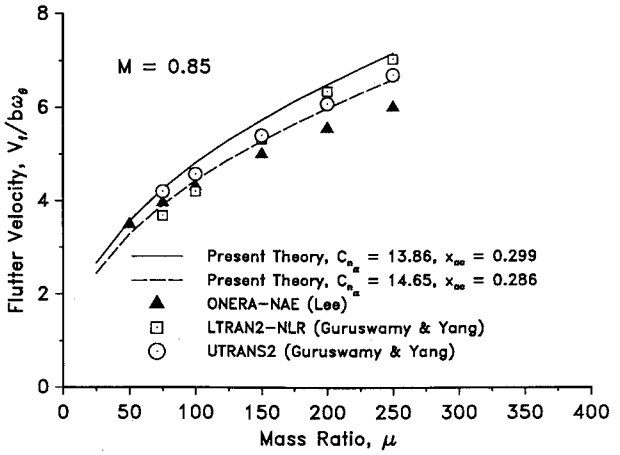

Fig. 8 Variation of flutter velocity with mass ratio at M = 0.85.

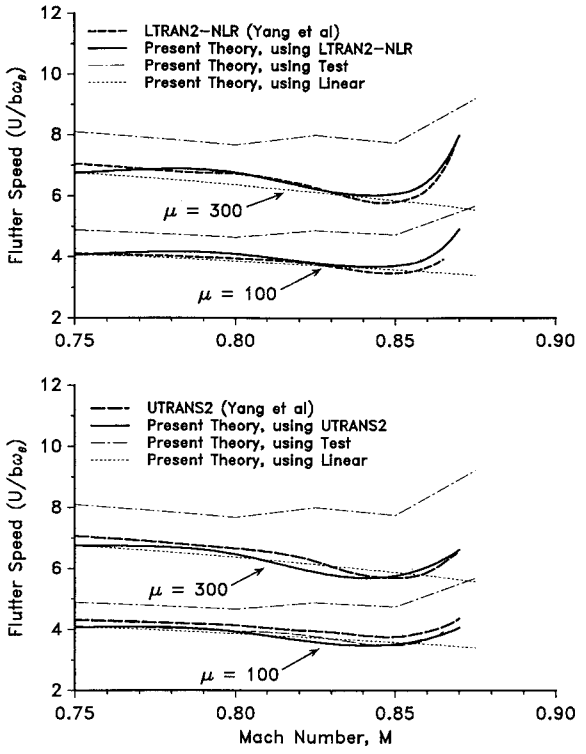

Fig. 9 Flutter boundary for the NACA 64A006 airfoil.

The determination of the transonic flutter boundary was also conducted in this study. The problem of determining the flutter boundary basically becomes a search for lowest speed for which ζ_k becomes positive. For the purposes of this calculation, values of the lift curve slope and aerodynamic center for the NACA 64A006 were derived from the experimental measurements given in Ref. 21, as well as from the static data computed by LTRAN2-NLR and STRANS2/UTRANS2 as given in Ref. 22.

Typical results for the flutter boundary are shown in Figs. 9, where the nondimensional flutter speed is plotted vs Mach number. Figure 9a presents the flutter boundary computed by STRANS2/UTRANS2 and the present method, using the following as inputs: 1) the static data from STRANS2/UTRANS2, 2) experimental data, and 3) conventional subsonic linear theory (x_{ac} = 0.25, $C_{N_\alpha} = 2\pi/\beta$). Figure 9b presents the flutter boundary computed by LTRAN2-NLR and the present method using the static data from LTRAN2-NLR. With conventional linear theory, the flutter speed decreases continuously with increasing Mach number. The decrease in flutter speed is a direct result of the increase in lift curve slope with increasing Mach number. When a Mach number dependent aerodynamic center is included, it is clear that the sudden aft movement in x_{ac} due to the developing supercritical flow is responsible for the rapid increase in the flutter speed. As other studies have noted, the transonic dip phenomena, a dip in the flutter speed at some critical speed, is a result of these two changes. This phenomena is well predicted by the present theory using $C_{N_\alpha}(M)$ and $x_{ac}(M)$ predicted by the CFD analyses. However, as shown in Fig. 3, the CFD analyses predict a significantly different aerodynamic center compared to the test data, and this is responsible for the different behavior seen in the flutter boundary.

IV. Conclusions

A method has been presented that quite adequately approximates the unsteady aerodynamics of an airfoil operating in transonic flow. The approach also allows the unsteady aerodynamics for arbitrary forcing to be described by a system of first-order ordinary differential equations, i.e., in state-space form. Validation has been conducted with CFD data for oscillating airfoils in transonic flows. The state equations governing the unsteady aerodynamic behavior of the airfoil have also been directly appended to the structural response equations. The resulting aeroelastic behavior of the airfoil section has been analyzed as a standard eigenvalue problem.

To illustrate the utility of the overall method, an aeroelastic analysis has been conducted on the NACA 64A006 airfoil in transonic flow. Values for the static lift curve slope and aerodynamic center on the airfoil for various Mach numbers were obtained from a CFD analysis as well as experimental measurements and used as the only input to the model. It was shown that the transonic dip phenomena is well predicted if the static lift curve slope and the aft moving aerodynamic center in transonic flow are properly represented.

It has been shown that flutter predictions are in good agreement with those calculated using more sophisticated nonlinear aerodynamic models. A significant improvement in predictive capability has been demonstrated compared to classical incompressible theory, but with only a moderate increase in computational effort. Flutter predictions using classical incompressible theory were significantly optimistic as compared to the CFD solutions, whereas the present method solutions compared quite well with the CFD results.

This method is not presented as a replacement for CFD-based transonic aeroelasticity analyses, but rather it is presented as an extremely cost effective way of obtaining the unsteady airloads in aeroelastic stability studies, particularly for preliminary design. The process of determining a typical flutter speed required only a few seconds of CPU time on a SUN 3/60 computer using eigenanalysis. In addition, only two coefficients are required to characterize an airfoil using this method, the static lift curve slope and the aerodynamic center offset. Although these must be determined for a range of Mach numbers, these data are typically required for even a simple quasisteady aeroelastic analysis and are readily obtainable.

Because of its generality for different Mach numbers, this method is particularly useful for the comprehensive aeroelastic analysis of helicopter rotors, where identification of the aerodynamic states is difficult or impossible. Furthermore, since constraints are not placed on the solution algorithm, the method is a useful enhancement to many existing codes for aeroelasticity and flutter analysis that may presently be based on incompressible flow assumptions.

Acknowledgments

The authors wish to thank Khanh Nguyen of NASA Ames Research Center for the many helpful technical discussions.

References

[1]Theodorsen, T., "General Theory of Aerodynamic Instability and the Mechanism of Flutter," NACA Rept. 496, 1935.

[2]Bisplinghoff, R. L., Ashley, H., and Halfman, R. L., *Aeroelasticity*, Addison-Wesley, Reading, MA, 1955.

[3]Ballhaus, W. F., and Bridgeman, J. O., "Numerical Solution Techniques for Unsteady Transonic Problems," AGARD Rept. 679, June 1980, pp. 16-1–16-24.

[4]Ballhaus, W. F., and Goorjian, P. M., "Computation of Unsteady Transonic Flows by the Indicial Method," *AIAA Journal*, Vol. 16, No. 2, 1978, pp. 117–124.

[5]Guruswamy, P., and Yang, T. Y., "Aeroelastic Time Response Analysis of Thin Airfoils by Transonic Code LTRAN2," *Journal for Computers and Fluids*, Vol. 9, No. 4, Dec. 1981, pp. 409–425.

[6]Rizzetta, D. P., "Time-Dependent Responses of a Two-Dimensional Airfoil in Transonic Flow," *AIAA Journal*, Vol. 17, No. 1, 1979, pp. 26–32.

[7]Edwards, J. W., Bennett, R. M., Whitlow, W., Jr., and Seidel, D. A., "Time-Marching Transonic Flutter Solutions Including Angle of Attack Effects," *Journal of Aircraft*, Vol. 20, No. 11, 1983, pp. 899–906.

[8]Isogai, K., "Numerical Study of Transonic Flutter of a Two-Dimensional Airfoil," National Aerospace Laboratory, Japan, TR-NAL-TR-617T, July 1980.

[9]Karpel, M., "Design for Active Flutter Suppression and Gust Alleviation Using State-Space Aeroelastic Modeling," *Journal of Aircraft*, Vol. 19, No. 3, 1982, pp. 221–227.

[10]Dowell, E. H., Bland, S. R., and Williams, M. H., "Linear/Nonlinear Behavior in Unsteady Transonic Aerodynamics," *AIAA Journal*, Vol. 21, No. 1, 1983, pp. 38–46.

[11]Ueda, T., and Dowell, E. H., "Flutter Analysis using Nonlinear Aerodynamic Forces," *Journal of Aircraft*, Vol. 21, No. 2, 1984, pp. 101–109.

[12]Leishman, J. G., and Nguyen K. Q., "State-Space Model for Unsteady Airfoil Behavior," *AIAA Journal*, Vol. 28, No. 5, 1990, pp. 836–844.

[13]Leishman, J. G., and Crouse, G. L., "A State-Space Model of Unsteady Aerodynamics for Flutter Analysis in a Compressible Flow," AIAA Paper 89-0022, Jan. 1989.

[14]Leishman, J. G., "Validation of Approximate Indicial Aerodynamic Functions for Two-Dimensional Subsonic Flow," *Journal of Aircraft*, Vol. 25, No. 10, 1988, pp. 914–922.

[15]Wagner, H., "Über die Entstehung des dynamischen Auftriesbes von Tragflügeln," *Zeitschrift für angewandte Mathematik und Mechanik*, Vol. 5, No. 1, 1925, pp. 17–35.

[16]Jones, R. T., "The Unsteady Lift of a Wing of Finite Aspect Ratio," NACA Rept. 681, 1940.

[17]Edwards, J. W., Ashley, H., and Breakwell, J. V., "Unsteady Aerodynamic Modeling for Arbitrary Motions," *AIAA Journal*, Vol. 17, No. 4, 1979, pp. 365–374.

[18]Beddoes, T. S., "Practical Computation of Unsteady Lift," *Vertica*, Vol. 7, No. 2, 1983, pp. 183–197.

[19]Mazelsky, B., "On the Noncirculatory Flow About a Two-Dimensional Airfoil at Subsonic Speeds," *Journal of the Aeronautical Sciences*, Vol. 19, No. 12, 1952, pp. 848–849.

[20]Magnus, R. J., "Calculations of Some Unsteady Transonic Flows About the NACA 64006 and 64A010 Airfoils," Air Force Flight Dynamics Lab., Wright-Patterson AFB, OH, TR-77-46, July 1977.

[21]Stivers, L. S., "Effects of Subsonic Mach Number on the Forces and Pressure Distributions on Four NACA 64A-Series Airfoil Sections at Angles of Attack as High as 28°," NACA TN-3162, March 1954.

[22]Yang, T. Y., Guruswamy, P., Stritz, A. G., and Olsen, J. J., "Flutter Analysis of a NACA 64A006 Airfoil in Small Disturbance Transonic Flow," *Journal of Aircraft*, Vol. 17, No. 4, 1980, pp. 225–232.

[23]Lee, B. H. K., "A Study of Transonic Flutter of a Two-Dimensional Airfoil using the U-g and p-k Methods," National Research Council of Canada, Rept. LR-615/NRC 23959, Nov. 1984.

[24]Yang, T. Y., and Chen, C. H., "Flutter and Time Response Analysis of Three Degree of Freedom Airfoils in Transonic Flow," Air Force Flight Dynamics Laboratory, Wright-Patterson AFB, OH, AFWAL-TR-81-3103, Aug. 1981.

[25]Tijdeman, H., "Some Remarks on Unsteady Transonic Flow," Contribution to the Round Table Discussion on Unsteady Aerodynamics of the AGARD Fluid Dynamics Panel, Göttingen, May 1975.

[26]Davis, S. S., and Malcolm, G. N., "Experimental Unsteady Aerodynamics of Conventional and Supercritical Airfoils," NASA TM 81221, August 1980.